

A Zero-Watermarking Against Large-Scale Cropping Attack



Jing Wang , Sellappan Palaniappan , and Bing He 

Abstract Considering the digital copyright protection of the color image, and aiming at the shortcomings of the existing color image zero-watermarking algorithms against various attacks including image information loss, e.g., cropping, rows and columns removal, and smearing, etc. A color image zero-watermarking algorithm based on quaternion fractional-order generalized Laguerre moments (QFr-GLMs) is proposed. The novelties of the proposed scheme are as follows: (1) QFr-GLMs are applied the first time in the digital copyright protection based on color image zero-watermarking scheme; (2) The proposed zero-watermarking scheme can efficiently resist traditional noisy and smoothing filter attacks, moreover, when the image is attacked by large-scale cropping or smearing, the proposed zero-watermarking scheme can still detect the watermark correctly; Simulation experimental results prove that the performance of the proposed scheme is superior to that of the graying-based and the single channel-based zero-watermarking schemes.

Keywords Quaternion algebra · Fractional-order generalized Laguerre moments · Zero-watermarking · Cropping attack

1 Introduction

As an effective image descriptor, orthogonal moments have been widely used in the fields of image processing and analysis such as image reconstruction, digital image watermarking and objection recognition. Orthogonal moments can be divided into continuous orthogonal moments like Zernike moments [1], orthogonal Fourier-Mellion moments [2] and Bessel-Fourier moments [3], or into discrete orthogonal moments. Compared with continuous orthogonal moments, the discrete orthogonal moments have better numerical stability because the image itself is digitalized and

J. Wang (✉) · S. Palaniappan
Malaysia University of Science and Technology, 47810 Petaling Jaya, Malaysia
e-mail: wang.jing@phd.must.edu.my

J. Wang · B. He
Weinan Normal University, Weinan 714000, China

there is no numerical approximation operation. In the regions of image processing and analysis, color images include more information than grayscale and binary images. Quaternion algebra based color image representation regards an image as a three-dimensional vector describing the components of the color image, which effectively uses the color information of different channels of the color image. For color images, quaternion algebra can be used to construct quaternion image moments. Many quaternion image moments, such as: quaternion polar harmonic Fourier moments (QPHFM) [4], and quaternion exponent-Fourier moments (QEFMs) [5], have been proposed by researchers using the existing orthogonal polynomials. In order to make the image description more stable and accurate, the related scholars extend the integer-order image moments to the fractional-order level, and propose the related fractional-order orthogonal moments, such as the fractional-order Chebyshev moments (Fr-CMs) [6], and fractional-order Zernike moments (Fr-ZMs) [7].

Nowadays, digital copyright protection of image content is a key issue to protect the rights of intellectual property for authors, due to those digital image data can be easily carried out manipulations. Digital watermarking is considered a vital copyright protection technique by embedding watermark (or a message) into the images. At present, in the field of digital watermarking, many scholars and researchers have focused on the research of zero watermarking. In recent years, zero watermarking technology has become a research hot-spot in the field of information security, due to it solves the contradiction between invisibility and robustness in traditional watermarking technology. Wen et al. [8] have proposed the concept of zero watermark for the first time in 2003, since then, the research on zero watermarking has been continuously expanded and enhanced, and more and more related academic research results have been applied in the field of digital copyright.

Inspired by the Fractional-order Generalized Laguerre Moments (Fr-GLMs) that can effectively extract local features of an image, in our work, we propose a novel zero-watermarking scheme, to protect the copyright of color images, based on Quaternion Fractional-order Generalized Laguerre Moments (QFr-GLMs). This scheme takes advantage of Region of Interest (ROI) feature-extraction of the QFr-GLMs to improve the robustness against large-scale cropping and smearing attacks in the process of image transmission. In addition, since the technique of quaternion algebra is introduced, compared with the graying-based and the single channel-based zero-watermarking schemes, the performance of our proposed scheme is more excellent in resisting conventional image processing attacks.

2 Definition and Calculation of QFr-GLMs

Firstly, the three components of a color image $f^{rgb}(x, y)$, $f_r(x, y)$, $f_g(x, y)$, and $f_b(x, y)$, correspond to three imaginary components of a pure quaternion. Therefore, an image $f^{rgb}(x, y)$ in RGB color space can be expressed by the following quaternion.

$$f^{rgb}(x, y) = f_r(x, y)i + f_g(x, y)j + f_b(x, y)k. \tag{1}$$

Secondly, the corresponding fractional-order generalized Laguerre moments (Fr-GLMs) can be defined as

$$S_{nm}^{(\alpha, \lambda)} = w \sum_{i=0}^{N-1} \sum_{j=0}^{N-1} f^{gray}(i, j) \bar{L}_n^{(\alpha_x, \lambda_x)}(x_i) \bar{L}_m^{(\alpha_y, \lambda_y)}(y_j), \tag{2}$$

where $f^{gray}(i, j)$ represents a grayscale digital image. For convenience, we map the original two-dimensional digital-image matrix to a square area of $[0, L] \times [0, L]$. Here, $L > 0$, $w = (L/N)^2$, $x_i = \frac{iL}{N}$, $y_j = \frac{jL}{N}$, $i, j = 0, 1, 2, \dots, N - 1$, and the normalized fractional-order generalized Laguerre polynomial (NFr-GLPs) $\bar{L}_n^{(\alpha, \lambda)}(x)$ can be recursively calculated as follows

$$\bar{L}_n^{(\alpha, \lambda)}(x) = (A_0 + A_1 x^\lambda) \bar{L}_{n-1}^{(\alpha, \lambda)}(x) + A_2 \bar{L}_{n-2}^{(\alpha, \lambda)}(x), \tag{3}$$

where $\bar{L}_0^{(\alpha, \lambda)}(x) = \sqrt{\frac{\omega^{(\alpha, \lambda)}(x)}{\Gamma(\alpha+1)}}$, $\bar{L}_1^{(\alpha, \lambda)}(x) = (1 + \alpha - x^\lambda) \sqrt{\frac{\omega^{(\alpha, \lambda)}(x)}{\Gamma(\alpha+2)}}$, $A_0 = \frac{2n+\alpha-1}{\sqrt{n(n+\alpha)}}$, $A_1 = \frac{-1}{\sqrt{n(n+\alpha)}}$, $A_2 = -\sqrt{\frac{(n+\alpha-1)(n-1)}{n(n+\alpha)}}$, $\omega^{(\alpha, \lambda)}(x) = \lambda x^{(\alpha+1)\lambda-1} \exp(-x^\lambda)$, $\alpha > -1$, $\lambda > 0$, $\lambda \in R^+$, and $\Gamma(\cdot)$ is the gamma function, for details, see Ref. [9].

Finally, the right-side QFr-GLMs of an original RGB color image in Cartesian coordinates are defined as

$$\begin{aligned} Q_{nm}^{(\alpha, \lambda)} &= w \sum_{p=0}^{N-1} \sum_{q=0}^{N-1} \bar{L}_n^{(\alpha_x, \lambda_x)}(x_p) \bar{L}_m^{(\alpha_y, \lambda_y)}(y_q) f^{rgb}(p, q) \mu \\ &= -\frac{1}{\sqrt{3}} \left[w \sum_{p=0}^{N-1} \sum_{q=0}^{N-1} \bar{L}_n^{(\alpha_x, \lambda_x)}(x_p) \bar{L}_m^{(\alpha_y, \lambda_y)}(y_q) (f_r + f_g + f_b) \right] \\ &\quad + \frac{1}{\sqrt{3}} k \left[w \sum_{p=0}^{N-1} \sum_{q=0}^{N-1} \bar{L}_n^{(\alpha_x, \lambda_x)}(x_p) \bar{L}_m^{(\alpha_y, \lambda_y)}(y_q) (f_r - f_g) \right], \\ &\quad + \frac{1}{\sqrt{3}} j \left[w \sum_{p=0}^{N-1} \sum_{q=0}^{N-1} \bar{L}_n^{(\alpha_x, \lambda_x)}(x_p) \bar{L}_m^{(\alpha_y, \lambda_y)}(y_q) (f_b - f_r) \right] \\ &\quad + \frac{1}{\sqrt{3}} i \left[w \sum_{p=0}^{N-1} \sum_{q=0}^{N-1} \bar{L}_n^{(\alpha_x, \lambda_x)}(x_p) \bar{L}_m^{(\alpha_y, \lambda_y)}(y_q) (f_g - f_b) \right] \end{aligned} \tag{4}$$

where $\mu = (i + j + k)/\sqrt{3}$ is the unit pure imaginary quaternion. The QFr-GLMs expressed in quaternions and the Fr-GLPs of single channels in traditional RGB color images are related as follows:

$$Q_{nm}^{(\alpha,\lambda)} = A + iB + jC + kD, \tag{5}$$

where $A = -\frac{1}{\sqrt{3}}[S_{nm}^{(\alpha,\lambda)}(f_r) + S_{nm}^{(\alpha,\lambda)}(f_g) + S_{nm}^{(\alpha,\lambda)}(f_b)]$,

$B = \frac{1}{\sqrt{3}}[S_{nm}^{(\alpha,\lambda)}(f_g) - S_{nm}^{(\alpha,\lambda)}(f_b)]$, $C = \frac{1}{\sqrt{3}}[S_{nm}^{(\alpha,\lambda)}(f_b) - S_{nm}^{(\alpha,\lambda)}(f_r)]$,

$D = \frac{1}{\sqrt{3}}[S_{nm}^{(\alpha,\lambda)}(f_r) - S_{nm}^{(\alpha,\lambda)}(f_g)]$.











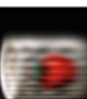
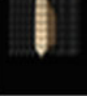
Accordingly, an original color image $f^{rgb}(p, q)$ can be reconstructed by finite-order QFr-GLMs. The reconstructed image is represented as

$$\begin{aligned} \bar{f}^{rgb}(p, q) &= w \sum_{p=0}^{N-1} \sum_{q=0}^{N-1} Q_{nm}^{(\alpha,\lambda)} \bar{L}_n^{(\alpha_x, \lambda_x)}(x_p) \bar{L}_m^{(\alpha_y, \lambda_y)}(y_q) \mu \\ &= -\frac{1}{\sqrt{3}} \left[w \sum_{p=0}^{N-1} \sum_{q=0}^{N-1} \bar{L}_n^{(\alpha_x, \lambda_x)}(x_p) \bar{L}_m^{(\alpha_y, \lambda_y)}(y_q) (B + C + D) \right] \\ &\quad + \frac{1}{\sqrt{3}} k \left[w \sum_{p=0}^{N-1} \sum_{q=0}^{N-1} \bar{L}_n^{(\alpha_x, \lambda_x)}(x_p) \bar{L}_m^{(\alpha_y, \lambda_y)}(y_q) (A + B - C) \right] \\ &\quad + \frac{1}{\sqrt{3}} j \left[w \sum_{p=0}^{N-1} \sum_{q=0}^{N-1} \bar{L}_n^{(\alpha_x, \lambda_x)}(x_p) \bar{L}_m^{(\alpha_y, \lambda_y)}(y_q) (A - B + D) \right] \\ &\quad + \frac{1}{\sqrt{3}} i \left[w \sum_{p=0}^{N-1} \sum_{q=0}^{N-1} \bar{L}_n^{(\alpha_x, \lambda_x)}(x_p) \bar{L}_m^{(\alpha_y, \lambda_y)}(y_q) (A + C - D) \right] \end{aligned} \tag{6}$$

3 Local-Feature-Extraction Analysis for QFr-GLMs

In this section, we develop the application of the QFr-GLMs to local-feature extraction from color images and the local feature image-cropping invariance of the QFr-GLMs is tested. The test images were four typical color images selected from the COIL-100 database, i.e., Toy, Bottle, Cup and Spoon size of 128×128 , respectively. The local features in each color image at different positions of the four-color images were reconstructed using the features extracted by the QFr-GLMs with different parameters. The experimental results are summarized in Table 1. This table shows that under different parameter settings, the proposed QFr-GLMs provided good image reconstructions in different regions of the original color image (the target areas of ROI extraction from the original color images are enclosed in the red-edged boxes). Under the parameter setting $\alpha_x = 22, \alpha_y = 1, \lambda_x = 1.4, \lambda_y = 1.6$, the QFr-GLMs extracted the upper part of the original color image. Meanwhile, the QFr-GLMs with $\alpha_x = 3, \alpha_y = 60, \lambda_x = 1.21, \lambda_y = 1.25$ extracted the bottom part of the original color image, those with $\alpha_x = 5, \alpha_y = 3, \lambda_x = 1.46, \lambda_y = 1$ obtained the left part

Table 1 Local-image reconstruction performances of the QFr-GLLMs

Original images				
The selected ROI images from original images				
The ROI reconstructed images				
Parameter values	$\alpha_x = 22, \alpha_y = 1,$ $\lambda_x = 1.40, \lambda_y = 1.60$ $L = 30, n = m = 20$			
	$\alpha_x = 3, \alpha_y = 60,$ $\lambda_x = 1.21, \lambda_y = 1.25$ $L = 30, n = m = 20$			
	$\alpha_x = 5, \alpha_y = 3,$ $\lambda_x = 1.46, \lambda_y = 1$ $L = 30, n = m = 18$			
	$\alpha_x = 1, \alpha_y = 100,$ $\lambda_x = 1.28, \lambda_y = 1.38$ $L = 30, n = m = 18$			

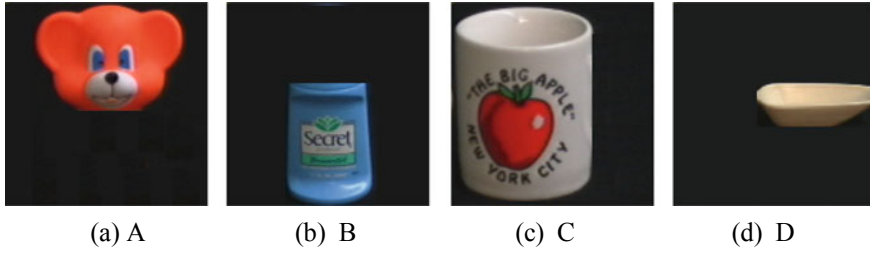


Fig. 1 The color cropped images at different positions from coil-100 datasets

Table 2 QFr-GLMs moduli and MRE for color cropped images at different positions

MRE	$ Q_{11}^{(\alpha,\lambda)} $	$ Q_{22}^{(\alpha,\lambda)} $	$ Q_{33}^{(\alpha,\lambda)} $	$ Q_{44}^{(\alpha,\lambda)} $	$ Q_{55}^{(\alpha,\lambda)} $	$ Q_{66}^{(\alpha,\lambda)} $	$ Q_{77}^{(\alpha,\lambda)} $	MAE
Toy	0.4135	1.9333	0.5847	1.4608	0.6005	0.8636	0.7116	–
A	0.4135	1.9333	0.5847	1.4608	0.6005	0.8636	0.7116	0
Bottle	0.3435	0.2851	0.6614	1.5392	0.7979	0.1921	0.3510	–
B	0.3435	0.2851	0.6613	1.5389	0.7972	0.1909	0.3485	0.0007
Cup	0.2371	1.4215	0.7482	1.6729	1.0414	0.6900	0.2739	–
C	0.2371	1.4215	0.7482	1.6729	1.0414	0.6900	0.2739	0
Spoon	0.0511	3.1356	0.0293	1.1299	0.1897	0.0869	0.0245	–
D	0.0511	3.1356	0.0291	1.1297	0.1903	0.0887	0.0246	0.0004

of the original color image, and those with $\alpha_x = 85$, $\alpha_y = 3$, $\lambda_x = 1.46$, $\lambda_y = 1.5$ extracted the right-upper part of the original color image. In addition, the image-cropping invariance of the QFr-GLMs is tested, and each of four-color images is cropped at different positions, respectively, which is illustrated in Fig. 1. The moduli for the QFr-GLMs of the four-color images are compared with those for the QFr-GLMs of the cropped images. The change rate of the moduli of the rotated images to that of the original images is measured by mean absolute error (MAE). The results in Table 2 shows that all MAE values are smaller than 0.0007, indicating that the moduli for the QFr-GLMs of the cropped images remain basically unchanged, which demonstrates that the QFr-GLMs under different parameter settings are invariant to image-cropping.

4 Proposed Zero-Watermarking Scheme

In this section, the QFr-GLMs were applied to zero-watermarking color image. Although the existing anti-geometric attack watermarking algorithms are effective against traditional geometric transformations (rotations, scaling, translations, or affine transformations) and conventional signal processing (noise adding, lossy

compression, and image filtering), the information loss from strong cropping and shearing attacks have been rarely investigated in this field. Some of the robust watermarking algorithms can extract the watermark information to a certain extent after weak cropping (information loss $< 25\%$), but cannot recover the watermark information after large-scale information loss (strong cropping or shear attacks). In such cases, the algorithms are invalid. To resolve these problems, we exploit the advantages of the proposed QFr-GLMs (local-feature extraction from color images and multi-point embedding) in a zero-watermarking system corrupted by large-scale cropping and smearing attacks.

4.1 Design of the Zero-Watermarking Scheme

The registration process of the proposed color-image zero-watermarking algorithm is shown as follows:

Step 1: Divide the original color host image needing copyright protection into $W \times W$ blocks. To preserve the details of the block image and reduce the false-alarm rate in digital watermarking, the size of the block image segmented in the host image should not be too small. Empirically, the size of the block image (if possible) should exceed $1/9$ of the original image size. In this paper, the color host image $I_{M \times N}^{(RGB)}$ was sized 192×192 . Therefore, we divided the original image into 3×3 blocks, and marked the segmented images as $B_k^{(RGB)}$.

Step 2: Extract the local-feature parameters (i.e., α_x , α_y , λ_x , λ_y , and L) of the color host image corresponding to each block image, and set them as the key character sequence $key_i = \{\alpha_x^i, \alpha_y^i, \lambda_x^i, \lambda_y^i, L^i\}$, $i = 1, 2, \dots, 9$. A number of lower-order moments of the proposed QFr-GLMs are then extracted as the feature vector $V_k^{(RGB)}$, $k = 1, 2, \dots, 9$. Here we set $V_k^{(RGB)} = \{v_{nm}^{(1)}, v_{nm}^{(2)}, \dots, v_{nm}^{(k)}, k = 9\}$, v_{nm} denote the lower-order moments of $Q_{nm}^{(\alpha, \lambda)}$ in Eq. (4). This feature vector is registered in the Certificate Authority Center (CA center, a third-party copyright protection center).

Step 3: The above information is time stamped and registered in the CA center, together with the user's signature information. At this time, the original color host image is announced to be under copyright protection.

4.2 Design of the Zero-Watermarking Detection System

Watermark detection is the reverse process of registration, in this stage, extracting the feature vector $\tilde{V}_k^{(RGB)}$ from the CA center, and sum the absolute differences between the feature vector $\tilde{V}_k^{(RGB)}$ obtained in the previous step and the feature vector $V_k^{(RGB)}$ obtained in the registration stage of the zero-watermarking algorithm. The sum is calculated as follows:

$$d = \min \left\{ \frac{1}{cnt^2} \sum_{n=1}^{cnt} \sum_{m=1}^{cnt} |v_{nm}^{(k)} - \tilde{v}_{nm}^{(k)}| \right\}. \quad (7)$$

In this experiment, $cnt = 10$ and $k = 1, 2, \dots, 9$. When $d \geq \varepsilon$ (where ε is an empirical threshold, set to 0.02 in the current experiment) and the time stamp does not match the information provided by the CA center, the verification is completed. The verification proves that the color host image either contains or lacks the watermark information.

4.3 Experimental Results of the Proposed Scheme

To verify the effectiveness of the zero-watermarking algorithm based on the proposed QFr-GLMs, the “cat” color image was extracted from the COIL-100 database, and its size was normalized to 192×192 . The size-normalized image was taken as the host image (see Fig. 2). This subsection describes the implementation and results of two groups of experiments. The first experiment investigated the robustness of the algorithm to various signal-processing. The second experiment examined the performance of the proposed zero-watermarking system on strongly cropped and randomly smeared images, and visualized the results of different cropping and smearing ratios on the cat host color image. In this subsection, the similarity between the original color host image and the attacked color image was measured by the *PSNR*, and the similarity between the detected feature vector $\tilde{V}_k^{(RGB)}$ and the feature vector $V_k^{(RGB)}$ in the CA center was judged by Eq. (4). Evidently, as d approaches 0, the zero-watermarking scheme becomes more robust.

Fig. 2 Original color host image of a cat ornament



Experiment 1. During network transmission, images are highly vulnerable to noise interference. In this experiment, the original color host image was tested under attacks by Gaussian white noise with a variance of 0.02, salt and pepper noise with a density of 5%, and speckle noise with a variance of 0.04. As noise interference is usually removed by filtering operations, filtering (with consequent loss of image pixels) is another frequently encountered attack in image processing and pattern recognition. In the experiment, the original color host image was subjected to median and average filtering with a 5×5 window. Furthermore, images in computer vision or signal processing are frequently processed by blurring and JPEG compression. Image blurring leads to partial block distortions, and JPEG compression causes pixel losses. During this experiment, the Gaussian blur parameter was set to the default in Matlab2013a’s software environment, and the JPEG compression ratio was set to 60. Table 3 compares the results of the proposed zero-watermarking scheme and other schemes (the direct graying-based method and the single channel-based method). The proposed algorithm was highly robust and outperformed the two established schemes.

Experiment 2. Cropping or smearing attacks are the most difficult problems in digital watermarking. Although the existing digital watermarking algorithms are robust to small-scale cropping and smearing operations, most of them fail under large-scale cropping or smearing operations. In this experiment, the color host image was cropped by different ratios (25%, 70%, 68%, and 82%) on different regions of the image. The image was also randomly smeared at ratios of 16%, 74%, and

Table 3 Typical results of images subjected to traditional image processing

Attacks	PSNR (dB)	<i>d</i>		
		Direct graying-based method [11]	Single channel-based method [12]	The proposed method
Gaussian white noise (Variance: 0.02)	17.82	0.0024	0.00157	0.00112
Salt and peppers noise (Density: 15%)	15.63	0.0043	0.00172	0.00121
Speckle noise (Variance: 0.04)	16.92	0.0025	0.00168	0.00099
Median filtering (Window: 5)	26.43	0.00038	0.00021	0.00018
Average filtering (Window: 5)	27.68	0.00022	0.00016	0.00011
Gaussian blur (Default)	28.22	0.00018	0.00013	0.00008
JPEG compression (Quality: 60%)	25.44	0.00029	0.00019	0.00014





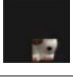
86%. Table 4 shows the cropped images and their experimental results. Unlike the zero-watermarking algorithm of Xia et al. [10], the proposed scheme based on the QFr-GLMs effectively detected the watermark, even on the image cropped by 82%. Thus, the proposed scheme is suitable for an image-copyright protection of cropped or smeared images.

5 Conclusions

This paper proposed a new zero-watermarking scheme, to protect color image copyright, based on QFr-GLMs. Our proposed scheme is very robust against traditional image processing, such as: noise, and smoothing filtering attacks, especially, against large-scale cropping and smearing attacks in the fields of image watermarking, which provide significant practical value in the copyright protection of color images. In future work, we would aim to address other research fields related to color images such as image retrieval, image classification, image matching and other research fields.





Funding This work was supported by the Science Foundation of the Shaanxi Key Laboratory of Network Data Analysis and Intelligent Processing (Grant No. XUPT-KLND201901), Shaanxi Province of Key R&D project (Grant No. 2020GY-051), Weinan regional collaborative innovation development research project (Grant No. WXQY001-001 and WXQY002-007) and Shaanxi Provincial Department of Education project (Grant No. 20JS044).

Table 4 Experimental results of images subjected to cropping and smearing attacks

Host image				
	$d = 0$			
Attacks	Parameters	Attacked color image	d	Detection results (Y/N)
Cropping	Upper-left cropping area: 25%		0	Y
Cropping	Rows cropping area: 70%		0.0082	Y
Cropping	Columns cropping area: 68%		0.0076	Y
Cropping	Upper-left Cropping area: 82%		0.0097	Y

(continued)

Table 4 (continued)

Host image				
	$d = 0$			
Attacks	Parameters	Attacked color image	d	Detection results (Y/N)
Smearing	Smearing area: 16%		0.0007	Y
Smearing	Smearing area: 74%		0.0128	Y
Smearing	Smearing area: 86%		0.03862	N

References

1. Singh, C., Ranade, S.K.: Image adaptive and high-capacity watermarking system using accurate Zernike moments. *IET Image Proc.* **8**(7), 373–382 (2014)
2. Singh, C., Upneja, R.: Accurate computation of orthogonal Fourier-Mellin moments. *J. Math. Imaging Vis.* **44**(3), 411–431 (2012)
3. Yang, T., Ma, J., Miao, Y., et al.: Quaternion weighted spherical Bessel-Fourier moment and its invariant for color image reconstruction and object recognition. *Inf. Sci.* **505**, 388–405 (2019)
4. Wang, C., Wang, X., Li, Y., et al.: Quaternion polar harmonic Fourier moments for color images. *Inf. Sci.* **450**, 141–156 (2018)
5. Wang, C.P., Wang, X.Y., Xia, Z.Q., et al.: Geometrically resilient color image zero-watermarking algorithm based on quaternion exponent moments. *J. Vis. Commun. Image Represent.* **41**, 247–259 (2016)
6. Benouini, R., Batioua, I., Zenkour, K., et al.: Fractional-order orthogonal Chebyshev moments and moment invariants for image representation and pattern recognition. *Pattern Recogn.* **86**, 332–343 (2019)
7. Chen, B., Yu, M., Su, Q., et al.: Fractional quaternion Zernike moments for robust color image copy-move forgery detection. *IEEE Access* **6**, 56637–56646 (2018)
8. Wen, Q., Sun, T.F., Wang, S.X.: Concept and application of zero-watermark. *Acta Electronica Sin.* **31**(2), 214–216 (2003)
9. Bhrawy, A.H., Alhamed, Y.A., Baleanu, D., et al.: New spectral techniques for systems of fractional differential equations using fractional-order generalized Laguerre orthogonal functions. *Fractional Calc. Appl. Anal.* **17**(4), 1137–1157 (2014)
10. Xia, Z.Q., Wang, X.Y., Zhou, W.J., et al.: Color medical image lossless watermarking using chaotic system and accurate quaternion polar harmonic transforms. *Signal Process.* **157**, 108–118 (2019)
11. Jin, N.R., Lv, X.Q., Gu, Y., et al.: Blind watermarking algorithm for color image in Contourlet domain based on QR code and chaotic encryption. *Packag. Eng.* **38**(15), 173–178 (2017)
12. Hong, Y.L., Qie, G.L., Yu, H.W., et al.: A contrast preserving color image graying algorithm based on two-step parametric subspace model. *Front. Inf. Technol. Electron. Eng.* **11**, 102–116 (2017)